June 2010 ISSN : 0974 - 7486 Volume 6 Issue 2

Trade Science Inc.

Materials Science

An Indian Journal

Full Paper

MSAIJ, 6(2), 2010 [142-149]

Hot dip aluminizing of 316l stainless steel on aluminuim and aluminuim-silicon alloys

A.A.Omar[1,2]*, M.M.Al-Aiat[3], S.I.Abdel-Aziz[3]

[1]Mechanical Engineering Department, Faculty of Engineering, TAIF University, El-Taif, El-Haweyah, P.O. Box 888, (KINGDOM OF SAUDI ARABIA)

[2]Mechanical Engineering Department, High Institute of Technology, Benha University, (EGYPT)

[3]Mechanical Engineering Department, Faculty of Engineering, Zagazig University, (EGYPT)

Received: 22nd March, 2010 ; Accepted: 1st April, 2010

ABSTRACT

316L stainless steel was coated by hot-dipping into commercially pure Al and two Al-Si alloys of 7%Si and 11.5% Si contents at dipping time varying from 1 to 60 min and temperatures ranging from 750 to 900ºC. Moreover, 5%Fe was added to each bath at 900°C. Microstructure observation, morphology of the alloy layer, element distribution, chemical composition and microhardness determination were performed by optical microscopy, scanning electron microscope (SEM) with an energy dispersive X-ray facility (EDX), and microhardness tester. The thickness of the intermetallic layer formed increases with increasing both the bath temperature and dipping time. Based on the experimental data, it is found that the largest and most uniform layer thickness was obtained at 800ºC and time 20 min in pure Al molten bath, and this is also the case when aluminizing in Al-11.5%Si molten bath, but when using Al-7%Si molten bath, the optimum dipping temperature was about 750°C also at time 20 min. The existence of Si reduces the intermetallic layer thickness and increases its microhardness. The addition of 5%Fe to the melt increases the layer thickness.

KEYWORDS

316L stainless steel;
Aluminizing;
Al-Si alloys;
Intermetallic layer;
Microhardness.

INTRODUCTION

Austenitic stainless steels are well known by its corrosion and oxidation resistance and, as a consequence, are extensively used in industrial applications such as petrochemical, nuclear, food and pharmaceutical industries[1]. Nevertheless, austenitic stainless steels lose their oxidation resistance at high temperatures due to decomposition of Cr_2O_3 invisible layer which protects the surface from high temperature oxidation[2].

Furthermore, austenitic stainless steels have poor tribological characteristics such as low hardness and wear resistance[3], and high friction coefficient, hence austenitic stainless steel is not the suitable select for some high temperature applications such as turbine blades, exhaust systems, and blankets for fusion reactors[2].

Different methods have been tried to modify the surface and overcome the weakness mentioned above without affecting the corrosion resistance, within these methods it was found hot dipping aluminizing[4].

In the aluminizing process, when wetting the surface of steel substrate, Al diffuses into steel[5] and many

diffusion reactions induce between the bath components and the elements of the substrate material[6] leading to the formation of an interlayer containing intermetallic phases[7,8].

The intermetallic alloy layer grows and dissolves concurrently into the molten aluminum alloy[9]. The growth and the dissolution rates of the intermetallic layer determine the thickness of the layer[10], in addition to dipping time, bath temperature, and chemical composition of the molten alloy[11-13].

Recent investigations show that the interface morphology, the growth mechanisms, the composition and the structure of these layers are like thickness affects the mechanical properties, the corrosion resistance and the surface quality of the final product[14].

The primary objective of this paper is to study and compare the composition, structure and growth properties of the intermetallic alloy layer produced on 316L austenitic stainless steel after hot dipping in molten aluminium bathes containing various amounts of silicon.

EXPERIMENTAL

Materials used

The substrate material used was 316L grade stainless steel, whose nominal chemical composition in wt% is (0.02 % C – 17.2% Cr – 10.2% Ni – 1.95% Mo – 0.98% Mn – 0.59% Si – 0.36% Cu).

The samples to be aluminized were cut from the sheet with average dimensions (25×20×2.5mm). For stress relief annealing, this steel was heated for 2 h at 900°C. Then these coupons were ground through 600-grit SiC paper and cleaned ultrasonically in ethanol.

Molten bath

The melts used are commercially pure Al and two Al-Si alloys, the compositions of these alloys are indicated in TABLE 1. Also in another set of experiments, 5% Fe powder is added to each melt at dipping temperature of 900ºC.

Sample preparation

Samples were degreased in a 100g/l sodium hydroxide solution at 50°C for 5 min, rinsed with water, and then descaled in aqua regia (3 HCL : 1 HNO3) at 25°C or 3 min, rinsed with water again and finally, ultrasonic cleaning in ethanol. As a final preparation, samples were immersed into potassium salt flux solution at 92°C for 2 min, and dried.

Aluminizing process

A 600g of each alloy was melted in graphite crucible in a resistance furnace, and maintained at different dipping temperatures, 750, 800, 850 and 900ºC.

Stainless steel samples were hanged by low carbon steel wires and dipped into the molten bath for different holding times ranging from 1 min to 60 min. Finally samples were pulled out from the melt and water quenched.

Microstructure and thickness measurement

For microstructure observation, the specimens were mounted with a cold setting resin, ground, polished, and etched with aqua regia to reveal the coating layers.

In order to measure the layers thickness, at least five photos were taken through optical microscopy at different places with equal spaces on each cross-section side, and 20 measurements of the thickness were evaluated from each photo and the mean value was calculated.

Microhardness measurement

The microhardness of the coated specimens was measured using MatsuZawa Vickers microhardometer with indentation load of 100 g for 20 s. The microhardness was evaluated by taking five indentations in each layer, and only the three middle values were averaged.

Energy dispersive x-ray analysis (EDX)

The element distributions of the coatings were analyzed using Jeol-Jsm5140 Scanning electron microscopy (SEM) with an energy dispersive X-ray facility (EDX).

RESULTS AND DISCUSSION

Microstructure changes of the layers

Pure Al molten bath

The cross section of the samples aluminized with pure Al (Figure 1(a)) shows the presence of two layers; intermetallic alloy layer, which is adjacent to steel,

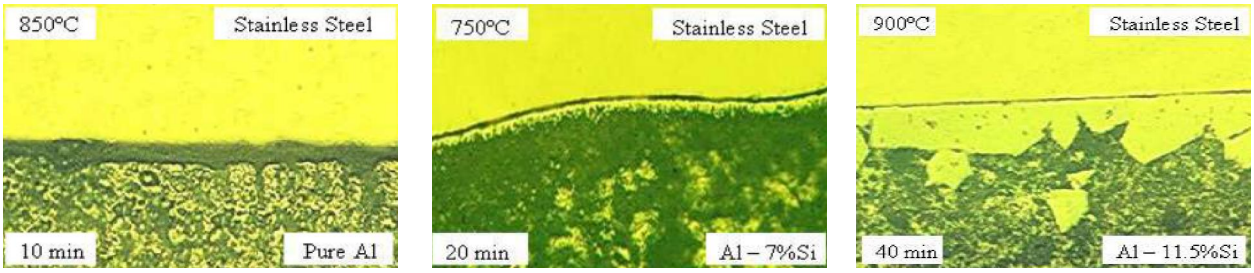

(a) (b) (c)

Figure 1 : Typical microstructure of the aluminized stainless stell (x200)

appears relatively compact, regular and good adhere with steel substrate, covered with topcoat outer layer adjacent to the melt, which is less homogeneous with porous structure. Unlike the tongue shaped morphology in aluminized carbon steel, the interface between the intermetallic alloy layer and the substrate appears flat.

Al – 7%Si molten bath

As seen in figure 1(b), the cross section of the aluminized steel specimens in Al-7%Si melt appears similar to that of samples aluminized with pure Al, except that the intermetallic layer composed of two sublayers. The upper sublayer, which is adjacent to the aluminum alloy topcoat, is much thicker than that of the lower sublayer that is adjacent to the steel substrate. However, in many cases it was difficult to distinguish between these two sublayers. Furthermore, the interface between the intermetallic layer and the steel substrate becomes smoother and more regular than in aluminizing with pure Al.

Al – 11.5%Si molten bath

According to figure 1(c), the upper sublayer becomes thicker and in many cases it takes faceted polyhedrons shapes as compared to samples aluminized in Al-7%Si melt, On the other hand, the thickness of lower intermediate layer that is adjacent to the steel substrate doesn't vary noticeably with the increase in Si content.

Effect of Si on alloy layer thickness

The intermetallic layer thickness decreases sharply when Al-7%Si alloy was used as dipping melt. Silicon effect can be recognized through three possible theories:

1 The first theory suggested that silicon inhibits the layer growth because Si decreases the diffusivity of Al in steel and enhances the rate of alloy layer dissolution in the melt[15].

2 The second theory concluded that the silicon effect arises from the formation of Fe-Al-Si ternary phases which nucleate and grow more slowly than η-Fe2Al5 (the main phase formed in aluminizing)[16].

3 The last theory deduced that Si preoccupies the large structural vacant sites on the C-axes of the orthorhombic cells of η-Fe2Al5 intermetallic compound, and this impedes aluminum atoms moving from molten Al to the steel substrate and inhibits the Fe2Al5 growth[17]. In addition to the retarding effect of silicon, we can see that silicon makes the surface of the Fe-Al alloy layer smooth and enhances the interfacial adhesion between the alloy coating layer and the steel substrate since there are no cavities or holes appear in the interface.

4 When Si content in the bath reaches 11.5%Si, the intermetallic layer thickness will increase again as seen in figure 2.

Effect of Fe on alloy layer thickness

The addition of 5%Fe to Al melt at 900ºC will decrease or completely prevent the dissolution of both the steel substrate and the alloy layer in the melt according to the degree of saturation of the melt, and as shown in figure 3, the intermetallic layer was much greater than obtained from aluminizing with commercially pure Al at the same dipping temperature and time. These results are in good agreement with some previous work[15,18,19].

It can be noticed from figure 3, that there are no great differences in the overall intermetallic layer thickness between the specimens aluminized in Al-7%Si molten bath with or without 5%Fe additions. This observation may be attributed to deduction that Si and Fe have contrary effect on the intermetallic layer thickness, and 5%Fe addition to the melt will annihilate the effect of 7%Si content in the melt. But we can see that adding

TABLE 1 : Nominal composition of molten alloys

Bath	Chemical composition (wt. %)					
	Si	Fe	Mg	Mn	Ti	Al
1	0.06	0.18	0.002	0.003	0.002	99.7
2	6.94	0.1	0.374	0.003	0.125	Bal.
3	11.5	0.12	0.251	0.004	0.139	Bal.

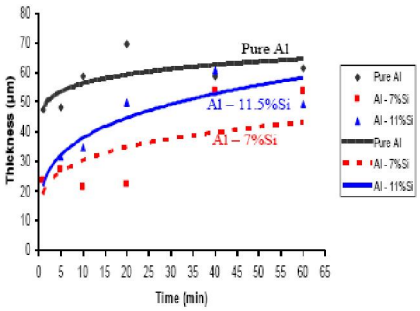

Figure 2 : Effect of dipping time and silicon content on the thickness of the intermetallic layer

5% Fe to the melt resulted in more smooth and uniform layer/substrate interface.

The microstructure shown in figure 3 and the curve illustrated in figure 4, reported that the intermetallic layer thickness is greater when aluminizing with Al-11.5%Si melt than when 5%Fe is added to the melt, this may be attributed to the assumption that the growth inhibition of 11.5%Si exceeds the growth enhancing of 5%Fe.

Effect of temperature and time on the intermetallic layer thickness

Both growth and dissolution of the intermetallic layer are affected by dipping time and temperature[20]. Generally, the effect of dipping time at different temperatures on the intermetallic layer thickness for all melts are the same as Fick's law of diffusion which describes that the thickness of intermetallic layer increases with dipping time at all dipping conditions[21,22].

The intermetallic layer grows relatively quick in the first few seconds, and then slows down as time increase up to 60 min, as outlined from figure 2, because the diffusion resistance of the intermetallic layer becomes larger with the increase in the intermetallic layer thickness, and also because the dissolution of the intermetallic alloy layer increases with time.

The effect of dipping temperature on the intermetallic layer thickness is somewhat complex especially in the case of aluminizing of stainless steel. The rise in temperature favors both the viscosity of the aluminium melt

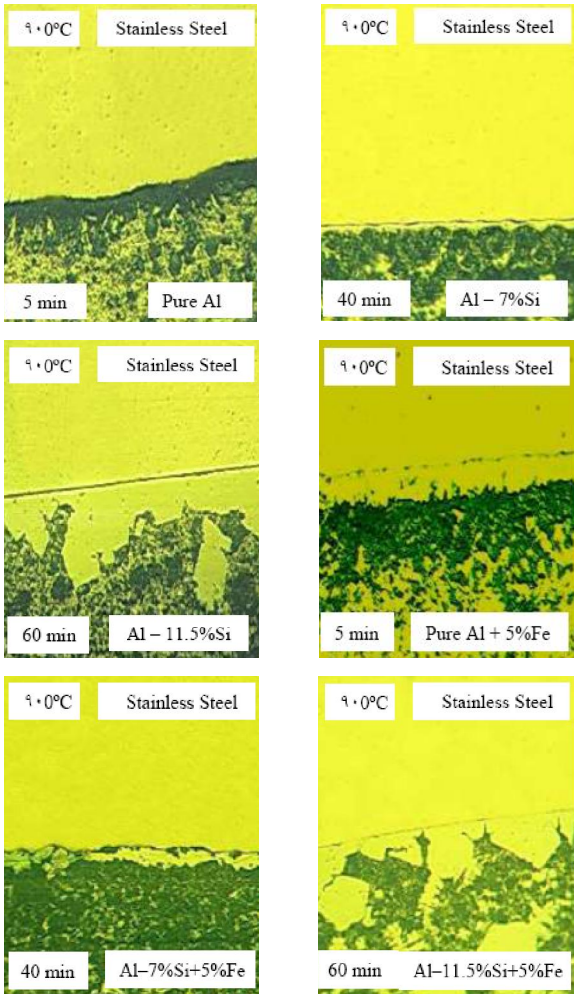

Figure 3 : Typical microstructure of the stainless steel samples aluminized at 900°C (x200)

and the diffusion of Al atoms from the melt toward the steel substrate and then the intermetallic layer thickness will increase. On the contrary, increasing the temperature results in an increase of the diffusion coefficient of transition metal (Fe, Cr, Ni, Ti, etc) into the melt, this will increases the solubility of theses elements in the molten Al, resulting in dissolution of the layer into the bath, giving a decrease in the layer thickness especially when the rate of dissolution exceeds that of layer growth.

Moreover, the presence of larger amounts of Cr and Ni in the molten Al due to the larger solubilities at higher dipping temperatures impedes the layer growth and decreases its thickness.

The rise in temperature favors both the viscosity of the aluminium melt and the diffusion of Al atoms from the melt toward the steel substrate and then the intermetallic layer thickness will increase.

On the contrary, increasing the temperature results

Full Paper

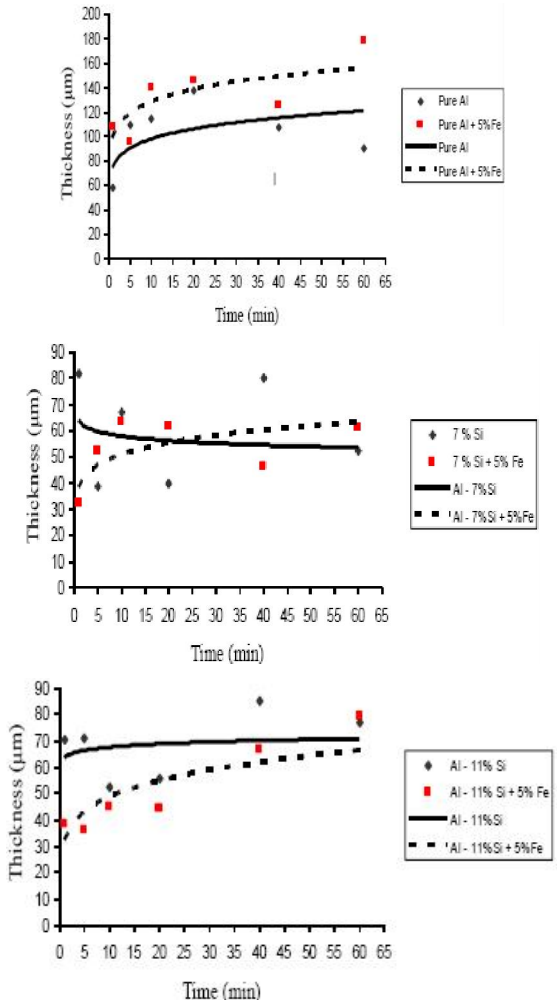

Figure 4 : Effect of Fe addition on the intermetallic layer thickness

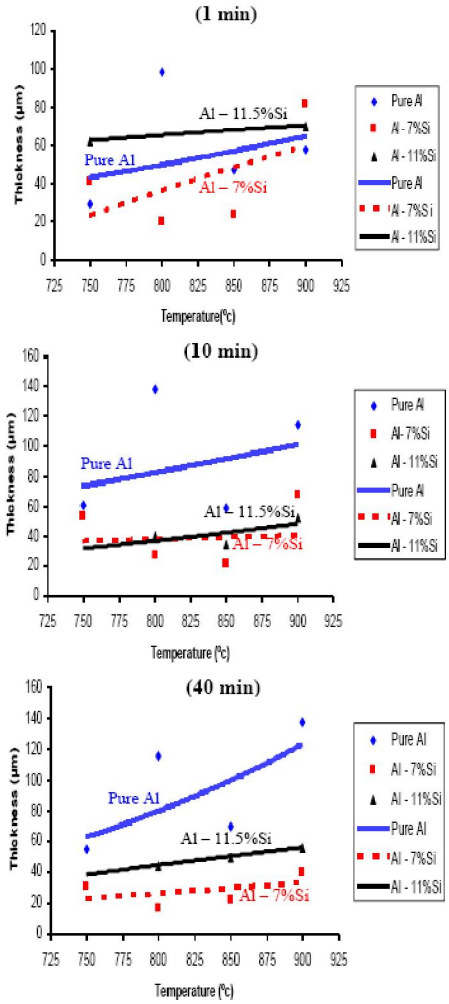

Figure 5 : The thickness of the intermetallic layer vs. temperature at different dipping times

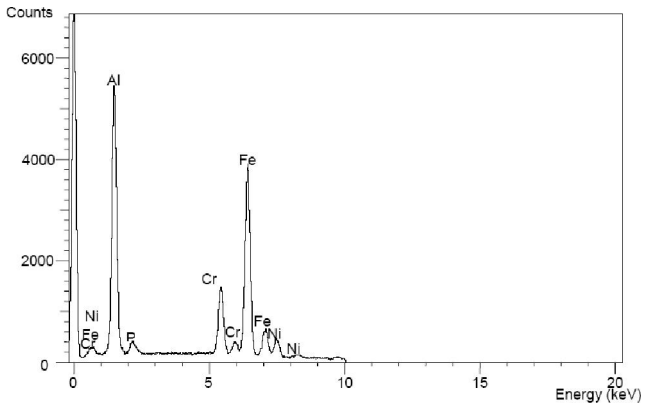

Figure 6 : EDX peaks showing the alloy layer of aluminized sample

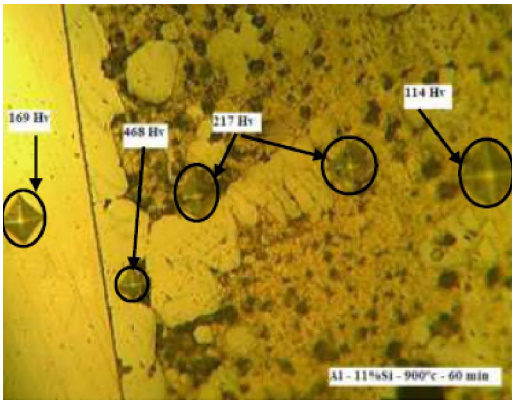

Figure 7 : Indentations of the measured micro hardness on the aluminized sample (x200)

in an increase of the diffusion coefficient of transition metal (Fe, Cr, Ni, Ti, etc) into the melt, this will increases the solubility of theses elements in the molten Al and this will increase the dissolution of the layer into the bath resulting in a decrease in the layer thickness especially when the rate of dissolution exceeds that of layer growth. Moreover, the presence of larger amounts of Cr and Ni in the molten Al due to the larger solubilities at higher dipping temperatures impedes the layer growth and decreases its thickness.

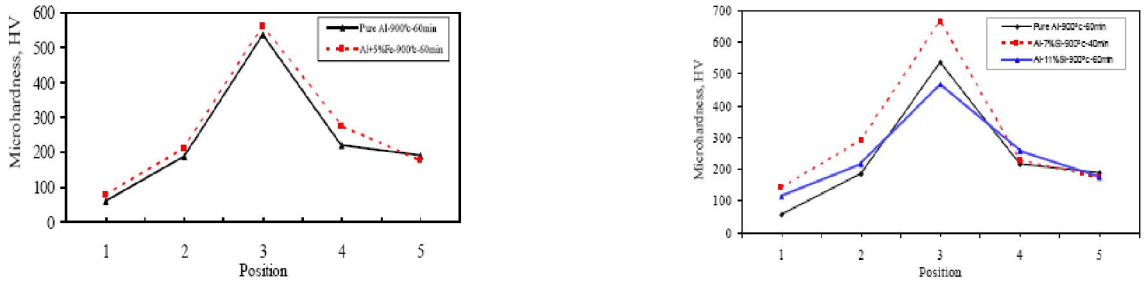

Figure 8 : Micro hardness profile of samples aluminized at 900°C for 60 min

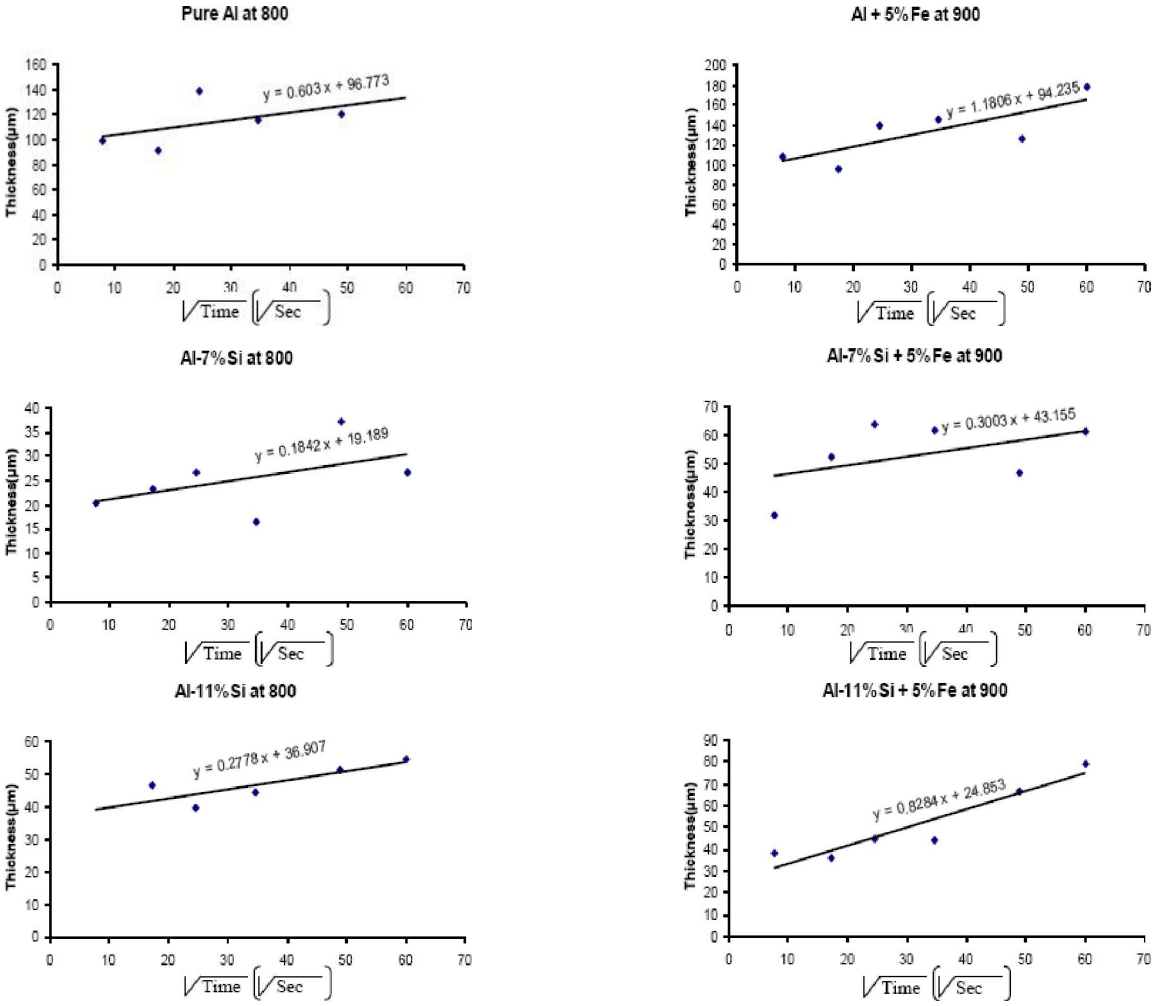

Figure 9 : The interface layer thickness vs. the square root of time for aluminized samples in different bathes at different temperatures

In figure 5, the intermetallic layer thickness is plotted versus temperature for various bath compositions and various dipping times, where it is obvious that the thickness of intermetallic layer generally increases with rising temperature.

When hot dipping in commercially pure Al molten bath, it is found that the largest and most uniform layer thickness was obtained at 800ºC and time 20 min, and this is also the case when aluminizing in Al-11.5%Si molten bath, but when using Al-7%Si molten bath, the dipping temperature was about 750ºC also at time 20 min.

Chemical analysis of the intermetallic layers

Based on TABLE 2, the gradients of Al and the steel elements (Fe, Cr and Ni) across the intermediate layer are different, the A1 content decreases from the top coat layer to the steel side, while the steel elements decrease in the opposite direction.

TABLE 2 : Results of EDX quantitative analysis

Pure Al – 900ºC – 60 min				
	Al	**Fe**	**Cr**	**Ni**
Base metal	-	65.6	25.7	5.8
Base metal /alloy layer interface	50.9	32.6	11.9	3.0
Alloy layer	59.6	26.4	10.0	2.3
Topcoat /alloy layer interface	62.6	24.6	8.7	2.4
Topcoat layer	79.9	12.4	4.6	1.0
Pure Al + 5%Fe – 900ºC – 60 min				
	Al	**Fe**	**Cr**	**Ni**
Base metal	-	66.1	26	5.7
Base metal /alloy layer interface	35.2	44.0	15.4	4.4
Alloy layer	37.8	43.1	13.9	4.2
Topcoat /alloy layer interface	41.8	36.9	15.0	4.3
Topcoat layer	44.9	37.4	11.6	3.9

TABLE 3 : Results of micro hardness measurements

Sample	Molten bath	Temp. (ºC)	Time (min)	Position 1	2	3	4	5
1	Al	900	60	57.5	185	536	217	189
2	Al + 5%Fe	900	60	76.9	209	560	274	176
3	Al - 7%Si	800	40	83.6	287	468	215	169
4	Al - 7%Si	900	40	142	290	665	228	174
5	Al - 7%Si + 5%Fe	900	60	165	292	542	245	182
6	Al - 11.5%Si	750	60	94.1	283	473	193	187
7	Al - 11.5%Si	850	40	111	256	464	228	192
8	Al - 11.5%Si	900	60	114	217	468	258	176
9	Al - 11.5%Si + 5% Fe	900	40	205	245	473	283	197
10	Al - 11.5%Si + 5%Fe	900	60	205	264	681	304	201

1: Top coat layer, 2: In outer layer near alloy later, 3: Inside alloy layer, 4: In base metal near alloy layer, 5: Base metal

The presence of Cr and Ni in the alloy layer and inside the top coat layer may be due to the dissolution of these elements from the base metal and the migration of these elements toward the melt direction.

The addition of 5%Fe to the melt resulted in increase in the concentration of some elements in the melt such as Fe, Cr, and Ni, while decrease the concentration of Al in the melt. This observation may be attributed to the formation of excess intermetallic compounds which consumes Al and in the same time increase of Cr, and Ni dissolution in the melt.

Figure 6 shows typical EDX peaks obtained for the intermetallic alloy layer for the aluminized specimen, indicating clearly the presence of Al in the alloy layer, but there is no Si observed in this analysis.

The absence of silicon peaks from the analyses may be attributed to two possible deductions:

1 The first deduction is that there are Fe-Al-Si intermetallic phases formed in hot dipping process but due to the neighboring of Si and Al in the periodic TABLE and consequently high Al peaks vanished the small Si peaks.

2 Another possible deduction suggests the absence of Fe-Si intermetallic in the alloyed layer may be due to the smaller atomic volume of Al rather than that of Si, then the diffusion rate of Al species is enhanced and Al-rich phases [particularly Fe2Al5] are expected to form directly in contact with the iron surface. The layer formed will prevent Si from reaching the base metal[23].

Microhardness distribution across the coating layers

The formation of intermetallic alloy layer lead to great increase in the microhardness more than the base metal[24]. TABLE 3 shows microhardness measurements for aluminized samples in different conditions.

As shown in figure 7, the microhardness values decreases when moving toward the topcoat layer due to the high aluminum content and the porous structure of the top coat layer, furthermore microhardness decrease still observed as moving toward base metal, and it may be accounted for the changes of the intermetallic phases.

The presence of silicon in the melt results in slight increase in the microhardness of both the intermetallic and top coat layers (Figure 8).

Moreover, the addition of 5%Fe powder to each molten bath results in noticeable increase in microhardness of both intermetallic layer and top coat layer, this may be due to the formation of harder intermetallic phases which give the higher microhardness of both layers.

Increasing dipping temperature and time leads to continuous formation of new hard phases, and therefore, increases the microhardness of intermetallic layer.

Aluminizing kinetics

In order to investigate the rate controlling mechanism and establish a kinetic law of the layer growth, the intermetallic layer thickness is plotted versus the square root of time and the results are fitted according to suitable relation[25].

As outlined in figure 9, the linear relationship between the thickness and $t_{1/2}$ is well displayed for all specimens, which confirms the solid state diffusion controlled growth of the intermetallic layer.

There are some cases where there are deviations from parabolic law due to scattering in experimental measurements of the alloy layer thickness.

CONCLUSIONS

1 An intermetallic layer formed on the steel substrate as a result of a reaction between the molten aluminum alloy and the steel substrate, the thickness of this layer increased with the increase in hot dipping temperature and time.

2 The presence of 7%Si in the melt decreases the diffusion rate of Al atoms toward the substrate, leading to a reduction of intermetallic layer thickness, but when Si content reaches 11.5% the thickness increases again.

3 The largest and most uniform layer thickness was obtained at 800ºC and time 20 min in pure Al molten bath, and this is also the case when aluminizing in Al-11.5%Si molten bath, but when using Al-7%Si molten bath, the dipping temperature was about 750ºC also at time 20 min.

4 The addition of 5% Fe to the melt increases very much the layer thickness when using pure Al bath, but Fe additions have no effect when aluminizing with Al-Si alloys.

5 The rate of growth for the intermetallic layer follows a near parabolic law; hence the mechanism responsible for the formation of this layer is solid state diffusion mechanism.

REFERENCES

[1] L.Karlsson; ESAB AB, **1**, 47-52 **(2004)**.

[2] F.Barbier, D.Manuelli, K.Bouche; Scripta Materialia, **36(4)**, 25-431 **(1997)**.

[3] W.Deqing, S.Ziyuan; Applied Surface Science, **227**, 255-260 **(2004)**.

[4] A.Bahadur; Materials and Manufacturing Process, **11(2)**, 335-232 **(1995)**.

[5] V.I.Dybkov; Journal of Materials Science, **25**, 3615-3633 **(1990)**.

[6] R.W.Richards, R.D.Jones, P.D.Clements, H.Clarke; International Materials Reviews, **39(5)**, 191-212 **(1994)**.

[7] H.Glasbrenner, O.Wedemeyer; Journal of Nuclear Materials, **257**, 274-281 **(1998)**.

[8] A.Bahadur, O.N.Mohanty; Materials Transactions, **32(11)**, 1053-1061 **(1991)**.

[9] W.Deqing, S.Ziyuan; Journal of Materials Science Letters, **22**, 1003-1006 **(2003)**.

[10] Z.Zhan, Y.He, D.Wang, W.Gao; Oxidation of Metals, **68**, 243-251 **(2007)**.

[11] S.Sharafi, M.R.Farhang; Surface and Coatings Technology, **200**, 5048-5051 **(2006)**.

[12] K.Barmak, V.I.Dybkov; Journal of Materials Science, **38**, 3249-3255 **(2003)**.

[13] R.Rajendran, S.Venkataswamy, U.Jaikrishna; Journal of Materials Science Letters, **22(8)**, **(2004)**.

[14] Y.Y.Chang, C.C.Tsaur, J.C.Rock; Surface and Coatings Technology, **200**, 6588-6593, **(2006)**.

[15] H.Glasbrenner, E.Nold, Z.Voss; Journal of Nuclear Materials, **249(1)**, 39-45 **(1997)**.

[16] G.Eggeler, W.Auer, H.Kaesche; Journal of Materials Science, **21**, 3348-3350 **(1986)**.

[17] H.Xiaoxia, Y.H.Z.Yan, P.Fuzhen; Materials Letters, **58**, 3424-3427 **(2004)**.

[18] P.Dillmann, B.Regad, G.Moulin; Journal of Materials Science Letters, **19(10)**, 907-911 **(2000)**.

[19] A.A.Abdel-Hamid, A.I.O.Zaid; 'Interaction of the Fe-25Cr-12Ni Superalloy with Molten Al and Properties of the Aluminized Layer', Production Engineering Design and Control (PEDAC'92) Conference, **1**, 45-57 **(1992)**.

[20] H.R.Shahverdi, M.R.Ghomashchi, J.Hejazi, S.Shabestari; Journal of Materials Processing Technology, **124**, 345-352 **(2002)**.

[21] K.Bouche, F.Barbier, A.Coulet; Materials Science and Engineering, A, **249(1-2)**, 167-175 **(1998)**.

[22] Y.Y.Cang, W.J.Cheng, C.J.Wang; Materials Characterization, (in press), **(2008)**.

[23] N.A.El-Mahallawy, M.A.Taha, M.A.Shady, A.R.El-Sissi; Materials Science and Technology, **13(10)**, 832-840 **(1997)**.

[24] C.J.Wang, S.M.Chen; Surface and Coatings Technology, **200**, 6601-6605 **(2006)**.

[25] H.R.Shahverdi, M.R.Ghomashchi, S.Shabestari, J.Hejazi; Journal of Materials Science, **37**, 1061-1066 **(2002)**.